coatings

MDPI

Article

Numerical Wear Analysis of a PLA-Made Spur Gear Pair as a Function of Friction Coefficient and Temperature

Gusztáv Fekete [1,2]

[1] Faculty of Sports Science, Ningbo University, Ningbo 315211, China
[2] Savaria Institute of Technology, Faculty of Informatics, Eötvös Loránd University, 9700 Szombathely, Hungary; fg@inf.elte.hu; Tel.: +36-(94)-504-460

Abstract: Polylactic acid (PLA)-made machine elements exhibit easy machining, biodegradability, and excellent mechanical properties. However, enhancing their wear resistance is still a crucial engineering point, which may be achieved by altering (lowering) their coefficient of friction (CoF). Therefore, the first aim of this paper is to analyze how wear is affected by the alteration of CoF. The second aim is connected to the fact that PLA is sensitive to heat, which also limits its applicability. Accordingly, the next goal is to explore the effect of temperature on wear propagation. This study answers these questions by means of multibody dynamics simulations of a PLA-made spur gear pair. Simulations were carried out under constant torque, while the CoF and the temperature were varied in a normal operation domain (CoF: 0.1–0.05, T = 20–30 °C). The results showed that the wear volume gradually began to decline at approximately 0.085 CoF, whilst convergence to steady-state wear could be observed at 0.05 CoF. In conclusion, alteration of the CoF can lower wear by 35%, in this specific domain, while even a 5 °C rise in temperature causes 40% wear progression. The feasibility of the numerical procedure was validated by comparing numerically and experimentally obtained wear–torque results.

Keywords: PLA; wear; multibody dynamics; Archard's law; gear pairs; friction; temperature

Citation: Fekete, G. Numerical Wear Analysis of a PLA-Made Spur Gear Pair as a Function of Friction Coefficient and Temperature. *Coatings* **2021**, *11*, 409. https://doi.org/10.3390/coatings11040409

Academic Editor: James Krzanowski

Received: 3 March 2021
Accepted: 29 March 2021
Published: 1 April 2021

1. Introduction

Three-dimensional (3D) printing has become probably the most dominant additive manufacturing process, combining CAD (Computer Aided Design) techniques and material science. Among printing materials, polylactic acid (PLA) is one of the most popular polyester used in desktop 3D printing due to its low cost, appropriate tensile strength, and biodegradability [1,2]. It has been applied not only in packaging and food service but in the agricultural [3], medical [4], and automotive sectors as well [5]. Due to the wide range of applications, especially in gear pairs, several articles have begun to focus on 3D-printed machine elements.

These studies are mainly experimental, and they can be divided into papers that deal with the material design approaches and those that set their focus on the applied production technologies to enhance the properties of PLA (or similar materials).

With regard to the material design direction, it is worth mentioning the work of Pawlak [6], who investigated how graphite influences the CoF and wear of PLA composites via a pin-on-disc platform. He concluded that graphite decreased the linear wear and CoF, while two optimum values were found in his compositions at 5 and 50%. In connection with the use of different agents to augment material properties, Lendvai and Brenn [7] blended thermoplastic starch with PLA via batchwise melt mixing with and without reactive compatibilization to enhance the interfacial adhesion. They succeeded in elevating the adhesion with different agents, and in the case of a chain extender, they achieved 20% higher yield strength as well.

The branch of PLA enhancements is slightly wider if production technologies are considered. Srinivasan et al. [8] and Chemezov et al. [9] paid much attention to specific

production settings, such as printing speed, printing temperature, bed temperature, and infill percentage, in order to enhance PLA's material properties in the case of simple pins and spur gears. Zhang et al. [10] performed wear rate tests on a custom-built gear wear test rig to differentiate manufacturing processes in the case of nylon-made spur gears. Their results showed that in some cases, better thermal behavior can be achieved by 3D printing technology than by injection molding.

As related to wear and frictional properties, Zhang et al. [11] provided a highly significant experimental evaluation of PLA materials; they analyzed different infill densities, printing directions, and load conditions. In their conclusions, they pointed out that the infill density (id) and CoF were directly proportional, except for an infill density of 25%.

It should be emphasized that three important research gaps have been found in the relevant literature:

1. No authors have attempted to identify a functional, mathematical link between PLA wear and CoF;
2. However, if such a link existed, it could be utilized to enhance the material properties;
3. Although Zhang et al. [11] provided data on the PLA temperature and CoF change as a function of time, tests were only carried out on a simple pin-on-disc configuration, without connecting the two phenomena.

Based on the above-mentioned points, first, it will be determined herein how wear changes as a function of the CoF to provide a possible link that can alter wear phenomena via appropriately chosen production technologies.

In the context of wear, CoF, and production technologies, it is worth noting an experimental study by Calvo et al. [12]. Their results explained how roughness parameters and the CoF correlated with each other. Although Calvo et al. [12] used a steel ball and titanium plate, their presented method and the idea could be generally applied. Within this context, Dangnan et al. [13] also provided results about the progression of the CoF, together with the roughness profile, in the case of Polyjet materials (namely, 3D Acrylonitrile butadiene styrene (ABS) and Verogray). Since the roughness directly depends on the production technologies used [14,15], an indirect, unsophisticated connection can be made between the technologies and the CoF. For example, if pure PLA has an average roughness height (R_a) of 10 μm and exhibits an average CoF of 0.2 ($\pm$0.1) [16], then this is equivalent to the achievable roughness of production processes such as snagging, sawing, forging, and, less frequently, extruding [17].

For this reason, the first novel aim of this paper lies in the following idea: if a numerical wear–CoF function is determined, then an appropriate average roughness height can be estimated. Based on the estimated roughness, the applicable manufacturing technology will ensure a suitable surface and the required low wear. It must be noted that no analytical or numerical study has pointed out or investigated this connection.

On the subject of the third research gap, it is worth mentioning that CoF and temperature have a particular connection with regard to PLA (or any similar biodegradable polyester). When a PLA-based specimen slides over a substantially abrasive surface, considerable heat is generated which needs to dissipate from the contact surface, causing not only elevated local temperature but wear as well [1]. This coupled phenomenon raises the question of how much wear is developed by temperature change, and whether is it possible to derive a function between the two phenomena.

Consequently, the second novel aim of this paper is to make a functional connection between temperature and wear propagation in PLA gear pairs if these factors are varied in the normal operation domain. Since such modelling was only carried out experimentally by Zhang et al. [11], with significantly simpler geometries, this further step in this topic holds significant relevancy.

The proposed aims are achieved by a numerical–analytical tool that can address wear propagation in PLA-made gear pairs by means of multibody dynamics (MBD) simulations.

2. Materials and Methods

2.1. Introduction of the Solution Concept

The first step is to formulate the problem by combining a differential-algebraic equation (DAE) system, which models the dynamics of the gear connection, with an ordinary differential equation (ODE) that describes the wear mechanism. To gain results from an MBD system, a DAE must be solved, which is generally defined in any MBD software as follows [18]:

$$\begin{bmatrix} \mathbf{M} & -\mathbf{D^T} \\ \mathbf{D} & 0 \end{bmatrix} \cdot \begin{bmatrix} \ddot{\mathbf{x}} \\ \boldsymbol{\lambda} \end{bmatrix} = \begin{bmatrix} \mathbf{f} \\ \boldsymbol{\gamma} \end{bmatrix} \quad (1)$$

where $\mathbf{M}$ denotes the mass matrix, $\mathbf{D}$ (and $-\mathbf{D^T}$) is the Jacobian matrix (and its transpose) of the constraint equations, $\ddot{\mathbf{x}}$ includes the acceleration (linear and angular) terms, $\boldsymbol{\lambda}$ is the Lagrange multiplier (representing the constraint and, more importantly, the contact forces), while $\mathbf{f}$ and $\boldsymbol{\gamma}$ are the external forces/moment torques and inertial terms, respectively. In this paper, the C++ base $\rightarrow$ d MSC.ADAMS software was used [19], which can simultaneously solve Equation (1) for $\ddot{\mathbf{x}}$ and $\boldsymbol{\lambda}$ if the geometry, material, constraints, and loads are properly defined. As a second step, when contact forces ($\boldsymbol{\lambda}$) are determined, an appropriate wear model must be chosen. In most cases, wear models are generally given in the form of a simple ODE [20]:

$$dW = f(F(t), s(t), k, \ldots). \quad (2)$$

In Equation (2), $F(t)$ represents the general load function, $s(t)$ represents the sliding length, and k denotes the specific wear rate with regard to the applied PLA material. Naturally, more parameters can be included into the model, and it is worth emphasizing that the presented method is generally applicable for other polymers (PDMS, PLGA, etc.) as well. When the contact forces are obtained from the MBD simulations (Equation (1)), they can be incorporated into the wear model (Equation (2)) to analyze wear propagation in the function of the CoF and the temperature. It must be mentioned that the two systems (the MBD and the ODE) can be solved separately.

2.2. Multibody Dynamics Simulation of a Spur Gear Connection

In MSC.ADAMS software, a spur gear pair was created via the 3D contact method (Figure 1a,b). This method allows geometry-based contact, while it calculates true backlash based on the actual working center distance and tooth thickness. In the connecting surfaces, no imperfections were considered. Later, wear efficiency was considered by the use of the specific wear rate.

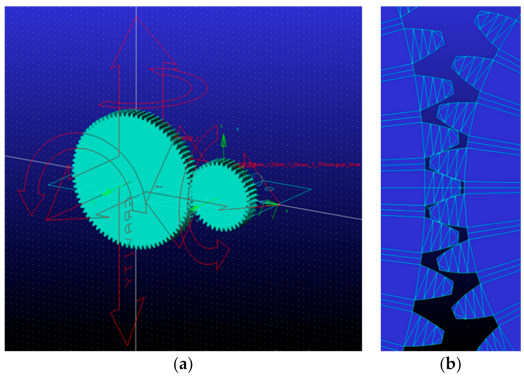

(a) (b)

Figure 1. Gear connection in MSC.ADAMS ((**a**) driver gear on the left, (**b**) driven gear on the right).

The main parameters of the two gears are shown in Table 1. The density of the PLA material can vary between 1000 and 2500 kg/m^3; however, here it was chosen to be 1250 kg/m^3, since a composition with this value is widely used in 3D printing [21].

Table 1. Gear parameters.

Parameters	Gear 1 (Driver)	Gear 2 (Driven)
Number of teeth	80	40
Module (mm)	1.35	1.35
Width (mm)	13	13
Involute	standard	standard
Addendum factor	1	1
Dedendum factor	1.25	1.25
Tip radius (R_{tip}) (mm)	55.35	28.35
Foot radius (R_{foot}) (mm)	52.31	25.3125
Tooth thickness (mm)	2.12	2.12
Density (kg/m^3)	1250	1250

The following boundary conditions were applied on the gears: Both of the gears were constrained by revolute joints in their centers of mass, which allowed rotation perpendicular to the working grid, but no translation. A general force vector was applied on the driver gear, which included a torque of 0.1 Nm, perpendicular to the working grid. This applied torque initiated the motion of the gear connection. Between the connecting gear teeth, contact constraints were defined, which considered the simple Coulomb's law. It must be noted that there are two possible ways to model contact constraints in MSC.ADAMS: by means of the impact function model or the Poisson restitution model [22]. In this paper, the impact function was applied, wherein friction forces are determined on a velocity-based approach. For friction calculations, four parameters need to be set for the simulation, namely, μ_{static}, $\mu_{kinetic}$, v_s (stiction transition velocity), and v_d (friction transition velocity). Default values were used for v_s and v_d, while the static and kinetic CoFs were changed during the simulations according to Table 2. It is relevant to note that MSC.ADAMS calculates the friction force using μ_{static} when two objects in contact exhibit zero relative velocity, while $\mu_{kinetic}$ is applied if the bodies exhibit nonzero relative velocity.

Table 2. Friction and temperature conditions during the simulations.

Conditions	μ_{static}	$\mu_{kinetic}$	Temperature
Friction condition no. 1	0.3	0.1	293/298/303 K (20 °C/25 °C/30 °C)
Friction condition no. 2	0.25	0.0825	293/298/303 K (20 °C/25 °C/30 °C)
Friction condition no. 3	0.2	0.066	293/298/303 K (20 °C/25 °C/30 °C)
Friction condition no. 4	0.15	0.05	293/298/303 K (20 °C/25 °C/30 °C)

The calculations were carried out on a Dell XPS laptop equipped with an i3-2310 CPU, 3 GB memory, and integrated HD Graphics 3000.

The simulation parameters were set as follows: complete simulation time: 0.1 s; time step: 1500. Four simulations were carried out, where the CoF ranged between 0.3 and 0.1 according to the typical PLA values [1,11], and the temperature between the gears was altered in each simulation to analyze its effect on wear propagation. One simulation lasted approximately 2 min. Since PLA becomes soft at around 70–80 °C, the investigation focused on a temperature zone where the polymer stays stable and which can be maintained by the use of simple cooling fans. The four simulation conditions are listed in Table 2.

During the simulations, the gears performed five complete revolutions; the aim of this was to investigate the running-in process in the gear connection where severe wear appears before it turns into steady-state wear [23].

2.3. Wear Modelling in Gear Pairs

Addressing wear (W) in a gear connection can be approached by simple augmentation of the Archard law [20], where F_C is the contact force and k is the specific wear rate. First, let us consider the law in its original form as a simple ODE:

$$\frac{dW}{ds} = k \cdot F_C(t). \tag{3}$$

This can be altered by re-arranging the law and breaking up ds as follows:

$$dW = k \cdot F_C(t) \cdot ds = k \cdot F_C(t) \cdot v_{sliding}(t) \cdot dt. \tag{4}$$

By the use of the well-known formula for sliding velocity between gear teeth, we obtain

$$v_{sliding}(t) = 2 \cdot \pi \cdot R \cdot (\omega_{driver}(t) + \omega_{driven}(t)) \tag{5}$$

where R is an approximation denoting equal distance between the pitch radius and the tip radius. This length also equals half the actual addendum (h_a):

$$R = \frac{h_a}{2} = \frac{R_{tip} + R_{tip}}{2} - \left(\frac{R_{tip} - \frac{R_{tip} + R_{tip}}{2}}{2} \right) = 7.6 \cdot 10^{-4}\ m. \tag{6}$$

It must be mentioned that $2 \cdot \pi$ is used since ω is acquired in rev/sec in MSC.ADAMS. Furthermore, we obtain the following wear equation:

$$dW = 2 \cdot \pi \cdot k \cdot R \cdot F_C(t) \cdot (\omega_{driver}(t) + \omega_{driven}(t)) \cdot dt. \tag{7}$$

In the last step, lubrication is considered in the contact, which can be described by the fractional film defect function (ψ) [24]:

$$\psi(t, T_s) = 1 - e^{-\left[\frac{\alpha_X}{v_{sliding}(t) \cdot t_0} \cdot e^{-\left[\frac{E_a}{R_g \cdot T_s}\right]}\right]} = 1 - e^{-\left[\frac{\alpha_X}{R \cdot (\omega_{driver}(t) + \omega_{driven}(t)) \cdot t_0} \cdot e^{-\left[\frac{E_a}{R_g \cdot T_s}\right]}\right]}. \tag{8}$$

The function depends on several parameters, listed in Table 3, where temperature (T_s) was varied in the calculation to observe its effect on wear. It is worth noting that the function can change between 0 and 1. The subsequent approximate wear propagation is defined as follows:

$$dW = 2 \cdot \pi \cdot k \cdot R \cdot F_C(t) \cdot \psi(t, T_s) \cdot (\omega_{driver}(t) + \omega_{driven}(t)) \cdot dt. \tag{9}$$

As a final step, the obtained numerical data ($F_C(t)$, $\omega_{driver}(t)$, $\omega_{driven}(t)$) were incorporated into Equation (9) and integrated in each time step as follows:

$$W = 2 \cdot \pi \cdot k \cdot R \cdot \psi(t, T_s) \cdot \int F_C(t) \cdot (\omega_{driver}(t) + \omega_{driven}(t)) \cdot dt + W_{initial}. \tag{10}$$

As a matter of course, the wear function could be extended by considering more parameters, e.g., the molecular weight, which can vary in a wide range. Although it is widely known that excessive heat will cause degradation in the molecular weight of PLA [25], in this analysis, only a certain, mild temperature zone was considered (between 20 °C and 30 °C), where this effect is negligible. The parameters of Equations (8) and (10) are listed in Table 3.

Table 3. Gear parameters.

Parameter	Quantity and Unit
k: specific wear rate [8]	65×10^{-5} (mm^3/Nm)
$\mu_{kinetic}$: coefficient of kinetic friction	Listed in Table 2.
$F_C(t)$: contact force function	Obtained from MBD simulation
$\omega_{driver}(t)$, $\omega_{driven}(t)$: angular velocities	Obtained from MBD simulation
dt: duration of motion	0.1 (s)
Ea: lubricant adsorption heat [24]	49×10^3 (J/mole)
t_0: fundamental time of vibration of a molecule in adsorbed state [24]	3×10^{-12} (s)
R_g: gas constant [24]	8.31 (J/mole K)
α_x: diameter of the area associated with an adsorb molecule [24]	3×10^{-10} (m)
Ts: surface temperature [24]	293/298/303 (Kelvin)

3. Results and Indirect Validation

3.1. Numerical Results

After the numerical integration of Equation (10), for each condition, the following results were achieved (shown in Figures 2–5).

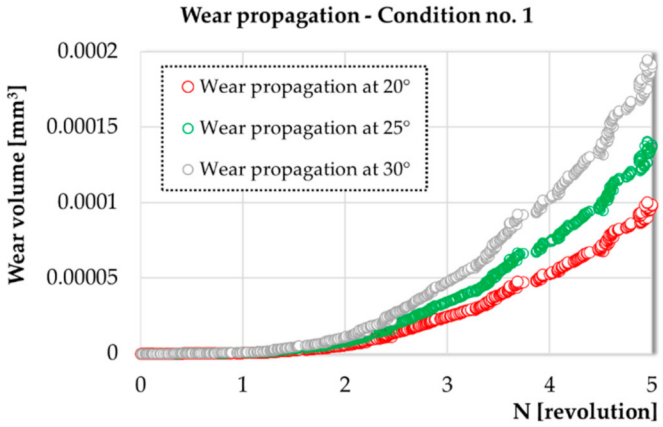

Figure 2. Wear propagation in the case of Friction Condition no. 1.

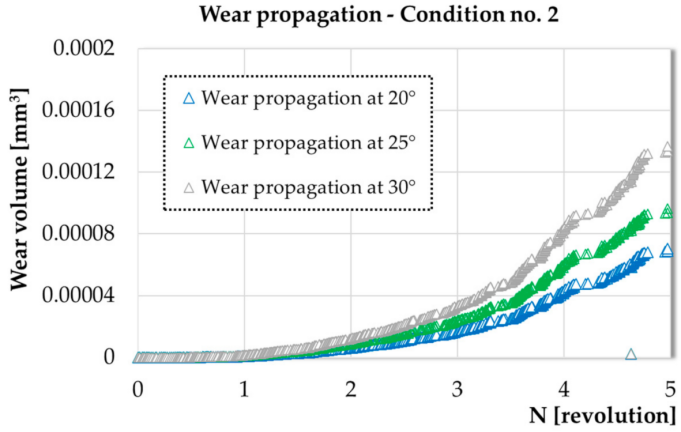

Figure 3. Wear propagation in the case of Friction Condition no. 2.

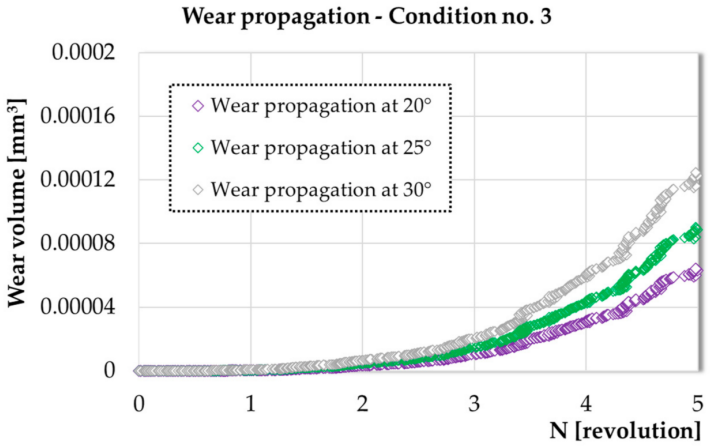

Figure 4. Wear propagation in the case of Friction Condition no. 3.

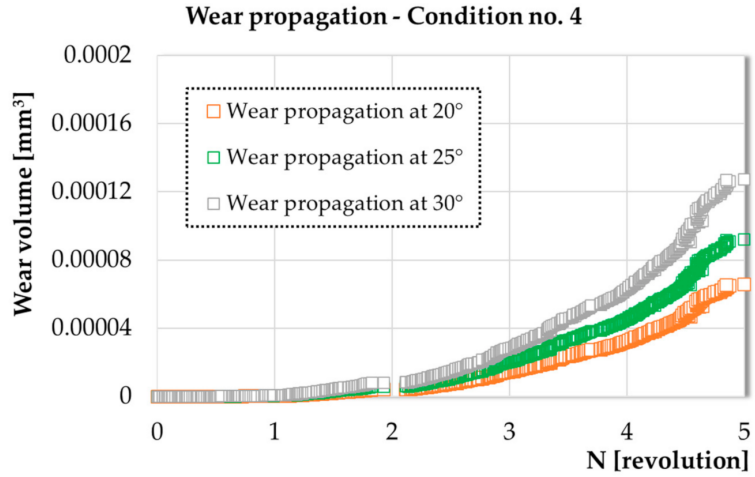

Figure 5. Wear propagation in the case of Friction Condition no. 4.

The maximum wear values at 20 °C were also investigated to obtain a global view of the effect of the kinetic CoF on wear. These results are displayed in Figure 6.

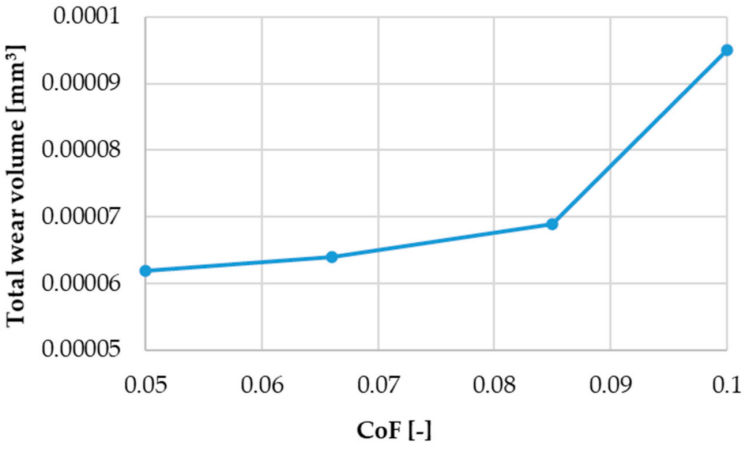

Figure 6. Wear propagation as a function of the kinetic coefficient of friction (CoF).

As expected, the highest friction combination (Condition no. 1) caused the highest wear as well. When the kinetic CoF was reduced by 15% in Condition no. 2, wear propagation decreased by 37.6% compared to that in Condition no. 1. Unusually, in the

following step, when friction was lowered again by 15%, only 7.8% wear decline was observed when the two following trends (Conditions 2 and 3) were compared. Between the last two conditions, there was only a 3.2% change in the wear volume, in spite of the CoF being decreased by another 15%. Therefore, it can be concluded that Condition no. 2 forms a threshold where the propagation slows down, and only a minor variation can be noted beyond it.

The effect of temperature was also investigated in a mild zone, where the molecular weight and the structure of the PLA texture do not change significantly. It was deduced that even low temperature had a considerable effect on wear (Figure 7).

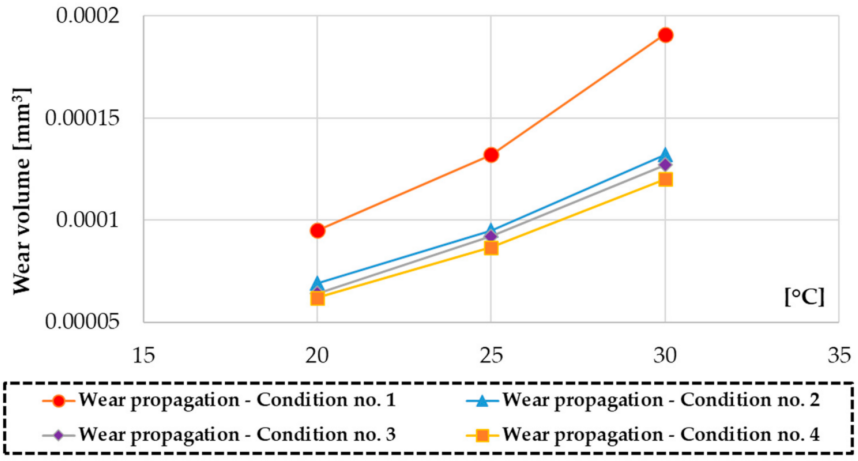

Figure 7. Wear propagation as a function of temperature.

A temperature rise of 5 °C (25% change in the numerical value of the temperature) caused approximately 40% more wear in the contact surfaces, while a temperature rise of 10 °C doubled the removed material. Therefore, it can be concluded that temperature elevation can be more crucial than the presence of a relatively high CoF.

What is highly important to note is that wear can be indirectly reduced by decreasing the roughness on the surface, which yields a lower CoF as well. Although additive technologies are mostly not fitting for the task of achieving a surface roughness between 0.1 and 0.5 µm (unlike milling, turning, grinding, or polishing) they can produce near-net-shape pieces, which can be further surface-finished in order to achieve an acceptable level of wear.

It must be added that with small nozzle diameter and layer height (0.3 and 0.2 mm, respectively), in some simple cases, 1 µm roughness could be achieved by fused deposition modeling (FDM), although this is only valid for one particular direction [26].

3.2. Indirect Validation

An indirect validation was also carried out in order to prove the reliability of the proposed numerical tool. Since, currently, no data are available on experimental wear modeling in the case of a PLA gear connection, a comparison with non-reinforced polyoxymethylene (POM) and 28% glass-fiber-reinforced polyoxymethylene (GFR POM)-made gear connections was chosen for verification [27]. POM behaves similarly to PLA in terms of several attributes; in addition, these materials are often blended to enhance their plasticity and general thermodynamic properties [28]. For the validation, identical numerical gear pairs were created (Figure 8a,b) in MSC.ADAMS according to the gear and material properties described in [27].

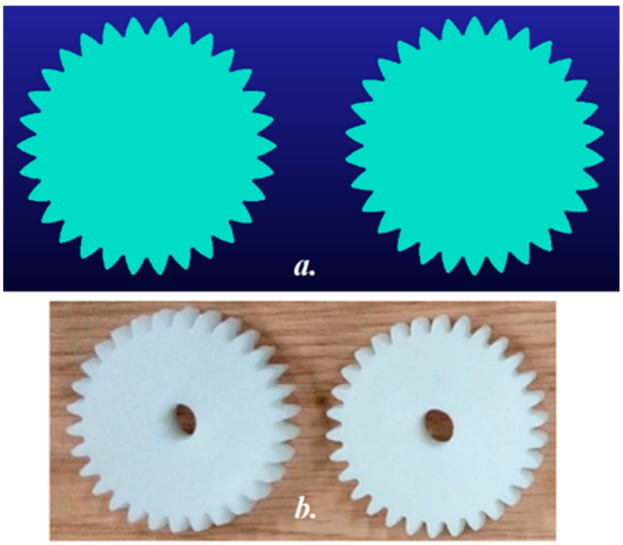

Figure 8. (**a**,**b**) Numerical models and real polyoxymethylene (POM)-made spur gears.

Subsequently, numerical simulations were carried with initial torque set at 6 Nm, which was increased by 1 Nm in each cycle up to 12 Nm, equivalent to the experiments. One cycle represented 20,000 rotations, while specific wear rates were defined as follows: $k_{POM} = 5.84 \times 10^{-6}$ mm^3/Nm, and $k_{GFR\text{-}POM} = 4.98 \times 10^{-6}$ mm^3/Nm [27].

When the literature data were compared to the numerically obtained ones, it was noted that the numerical solution followed, with slight overestimation, the evolution of the experimental wear propagation (Figure 9).

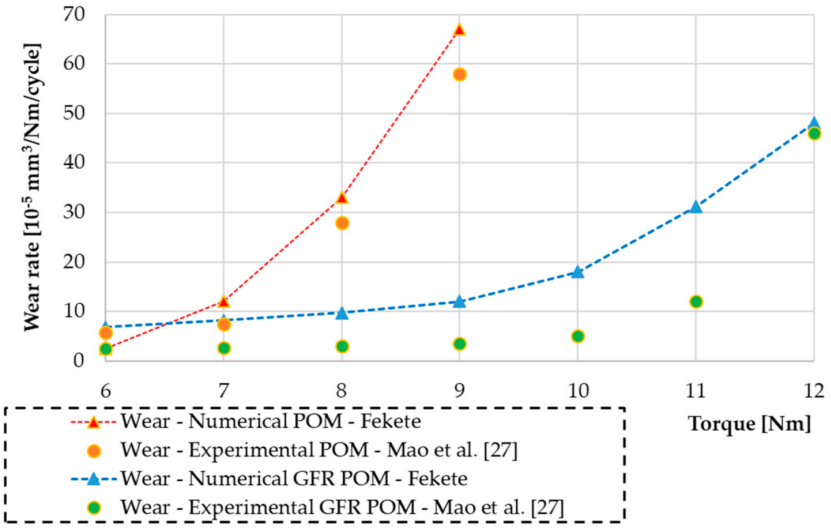

Figure 9. Comparison of experimental and numerical wear rates in the case of POM and glass-fiber-reinforced (GFR) POM gear pairs.

Based on the obtained results, it can be concluded that since the proposed numerical model can adequately estimate wear propagation in the case of POM-made materials, it is suitable for determining wear propagation in the case of PLA-based machine elements, such as gear pairs, as well.

4. Conclusions and Discussion

To conclude, a new wear model (a combination of MBD and an ODE) was presented that enables us to address wear propagation between spur gears, considering PLA or any similar composite material. The presented model placed emphasis on the effects

of friction and temperature by investigating several friction values and including the fractional film defect function. In consequence, the obtained results showed that the wear volume gradually began to decline approximately at 0.085 CoF, while a convergence to steady-state wear could be observed at 0.05 CoF. In summary, change in the coefficient of kinetic friction can lower wear by approximately 40% in this specific domain. On the other hand, it was also demonstrated that temperature had a more robust effect on the evolution of wear, since a 5 °C temperature rise (25% change in the numerical value of temperature) elevated wear by approximately 40%, while a 10 °C temperature rise (a further 25% change) virtually doubled the wear volume loss compared to that in the original state. Therefore, temperature proved to be a more crucial factor in the case of PLA-made spur gears than CoF; thus, proper cooling material or a ventilating system should be considered to enhance the operation time of these machine elements. It should also be mentioned that the obtained numerical results are based on certain geometrical assumptions with regard to the tooth connections—to obtain the sliding length—and the estimated values of the coefficients of friction and specific wear rates. More accurate theoretical calculations, e.g., those including the infill density, could significantly enhance the accuracy of the wear modelling, since it was demonstrated by Srinivasan et al. [8] that as the infill density increases, so begins a decrease in the specific wear rate. More importantly, Zhang at al. [11] revealed that the infill density and coefficient of friction are directly proportional; therefore, they can be expressed as a mathematical function. The inclusion of a CoF(id) function into the Archard law can be considered a next step to model the wear propagation of PLA or similar materials. On the other hand, further experimental studies to monitor wear and friction functions are also planned with a similar test rig to those described by Keresztes et al. [29] and Kalácska et al. [30].

Author Contributions: Conceptualization, methodology, software, validation, writing and visualization: G.F. Author have read and agreed to the published version of the manuscript.

Funding: This research was funded by the Key Project of the National Social Science Foundation of China (19ZDA352), the National Natural Science Foundation of China (No. 81772423), the NSFC-RSE Joint Project (81911530253), the National Key R&D Program of China (2018YFF0300903, 2018YFF0300905), and the K. C. Wong Magna Fund of Ningbo University.

Data Availability Statement: No new data were created or analyzed in this study. Data sharing is not applicable to this article.

Acknowledgments: This study was supported by Eötvös Loránd University and Ningbo University.

Conflicts of Interest: The author declares no conflict of interest. The funders had no role in the design of the study; in the collection, analyses, or interpretation of data; in the writing of the manuscript; or in the decision to publish the results.

References

1. Roy, R.; Mukhopadhyay, A. Tribological studies of 3D printed ABS and PLA parts. *Mater. Today Proc.* **2021**, *41*, 856–862. [CrossRef]
2. Sood, R.; Pradhan, S.K. Design and development of a low-cost open-source 3D printer and its single response optimization using polylactic acid (PLA) material. *Mater. Today Proc.* **2020**, *27*, 2981–2991. [CrossRef]
3. Knoch, S.; Pelletier, F.; LaRose, M.; Chouinard, G.; Dumont, M.-J.; Tavares, J.R. Surface modification of PLA nets intended for agricultural applications. *Colloids Surf. A Physicochem. Eng. Asp.* **2020**, *598*, 124787. [CrossRef]
4. Ali, W.; Mehboob, A.; Han, M.-G.; Chang, S.-H. Effect of fluoride coating on degradation behaviour of unidirectional Mg/PLA biodegradable composite for load-bearing bone implant application. *Compos. Part A Appl. Sci. Manuf.* **2019**, *124*, 105464. [CrossRef]
5. Motru, S.; Adithyakrishna, V.H.; Bharath, J.; Guruprasad, R. Development and evaluation of mechanical properties of biodegradable PLA/flax fiber green composite laminates. *Mater. Today Proc.* **2020**, *24*, 641–649. [CrossRef]
6. Pawlak, W. Wear and coefficient of friction of PLA-graphite composite in 3D printing technology. In Proceedings of the 24th International Conference of Engineering Mechanics, Svratka, Czech Republic, 14—17 May 2018; pp. 649–652.
7. Lendvai, L.; Brenn, D.; Mechanical, D. Morphological and thermal characterization of compatibilized poly(lactic acid)/thermoplastic starch blends. *Acta Tech. Jaurinensis* **2020**, *13*, 1–13. [CrossRef]
8. Srinivasan, R.; Aravindkumar, N.; Krishna, S.A.; Aadhishwaran, S.; George, J. Influence of fused deposition model-ling process parameters on wear strength of carbon fibre PLA. *Mater. Today Proc.* **2020**, *27*, 1794–1800. [CrossRef]

9. Chemezov, D.; Zubatov, D.; Vakhromeev, E.; Shchetnikov, V.; Goremykin, V.; Kuznetsov, A.; Zavrazhnov, D. Vladimir industrial college surfaces quality of plastic gears made by 3D printing. *Theor. Appl. Sci.* **2019**, *78*, 522–529. [CrossRef]
10. Zhang, Y.; Purssell, C.; Mao, K.; Leigh, S. A physical investigation of wear and thermal characteristics of 3D printed nylon spur gears. *Tribol. Int.* **2020**, *141*, 105953. [CrossRef]
11. Zhang, P.; Hu, Z.; Xie, H.; Lee, G.-H.; Lee, C.-H. Friction and wear characteristics of polylactic acid (PLA) for 3D printing under reciprocating sliding condition. *Ind. Lubr. Tribol.* **2019**, *72*, 533–539. [CrossRef]
12. Calvo, R.; D'Amato, R.; Gómez, E.; Ruggiero, A. Experimental analysis of the surface roughness in the coefficient of friction test. *Procedia Manuf.* **2019**, *41*, 153–160. [CrossRef]
13. Dagnan, F.; Espejo, C.; Liskiewicz, T.; Gester, M.; Neville, A. Friction and wear of additive manufactured polymers in dry con-tact. *J. Manuf. Process.* **2020**, *59*, 238–247. [CrossRef]
14. Zhang, X.; Chen, L. Effects of laser scanning speed on surface roughness and mechanical properties of aluminum/Polylactic Acid (Al/PLA) composites parts fabricated by fused deposition modeling. *Polym. Test.* **2020**, *91*, 106785. [CrossRef]
15. Andó, M.; Birosz, M.; Jeganmohan, S. Surface bonding of additive manufactured parts from multi-colored PLA materials. *Measurement* **2021**, *169*, 108583. [CrossRef]
16. Nedić, B.; Slavković, L.; Đurić, S.; Adamović, D.; Mitrović, S. Surface Roughness Quality, Friction and Wear of Parts Obtained on 3D Printer. In Proceedings of the Engineering Sciences, Faculty of Engineering, University of Kragujevac, Kragujevac, Serbia, 15–17 May 2019; Volume 1, pp. 98–103.
17. Black, J.T.; Kosher, R.A. *Materials and Processes in Manufacturing*, 10th ed.; John Wiley & Sons: Hoboken, NJ, USA, 2008.
18. Flores, P. *Concepts and Formulations for Spatial Multibody Dynamics*; Springer International Publishing: Berlin/Heidelberg, Germany, 2015.
19. MSC Software. Available online: https://www.mscsoftware.com/product/adams (accessed on 18 March 2021).
20. Archard, J.F.; Hirst, W. The wear of metals under unlubricated conditions. *Proc. R. Soc. London. Ser. A Math. Phys. Sci.* **1956**, *236*, 397–410.
21. Gunasekaran, K.; Aravinth, V.; Kumaran, C.M.; Madhankumar, K.; Kumar, S.P. Investigation of mechanical properties of PLA printed materials under varying infill density. *Mater. Today Proc.* **2020**. [CrossRef]
22. MSC Software, ADAMS/Solver. 2010, p. 35. Available online: http://simcompanion.mscsoftware.com/infocenter/index?page=content&id=DOC9391 (accessed on 18 March 2021).
23. Van Beek, A. *Advanced Engineering Design—Lifetime Performance and Reliability*; Delft University of Technology: Delft, The Netherlands, 2009.
24. Masjedi, M.; Khonsari, M. On the prediction of steady-state wear rate in spur gears. *Wear* **2015**, *342–343*, 234–243. [CrossRef]
25. Choi, J.-H.; Seo, W.-Y. Coloration of poly(lactic acid) with disperse dyes. Comparison to poly(ethylene terephthalate) of dyeability, shade and fastness. *Fibers Polym.* **2006**, *7*, 270–275. [CrossRef]
26. Alsoufi, M.S.; Elsayed, A.E. How surface roughness performance of printed parts manufactured by desktop FDM 3D printer with PLA+ is influenced by measuring direction. *Am. J. Mech. Eng.* **2017**, *5*, 211–222.
27. Mao, K.; Greenwood, D.; Ramakrishnan, R.; Goodship, V.; Shrouti, C.; Chetwynd, D.; Langlois, P. The wear resistance improvement of fibre reinforced polymer composite gears. *Wear* **2019**, *426–427*, 1033–1039. [CrossRef]
28. Zhang, G.; Qiu, J.; Sakai, E.; Zhou, Z. Interface investigation between dissimilar materials by ultrasonic thermal welding by the third phase. *Int. J. Adhes. Adhes.* **2021**, *104*, 102722. [CrossRef]
29. Keresztes, R.; Zsidai, L.; Kalácska, G.; Andó, M.; Lefánti, R. Friction of polymer/steel gear pairs. *Mech. Eng. Lett.* **2008**, *1*, 97–105.
30. Kalácska, G.; Kozma, M.; Debaets, P.; Keresztes, R.; Zsidai, L. Friction and wear of engineering polymer gears. In Proceedings of the World Tribology Congress III, Washington, DC, USA, 12–16 September 2005; Volume 1, pp. 259–260.